Appendix A: Nomenclature

Symbols

Symbol	Description	Unit
v	The velocity	*[m/s]*
h	The height	*[m]*
α_w	Roughness length parameter in the current wind direction	
P	The power	*[Watt]*
$\phi(v)$	Weibull's expression for probability density depending on the wind	
k	Shape parameter.	
c	Scale factor	
$\overline{v}$	The average velocity.	*[m/s]*
A_r	The rotor swept area	*[m^2]*
r	The radius of the rotor	*[m]*
ρ	Density of dry air (measured at average atmospheric pressure at sea level at 15° C)	*[kg/m^3]*
M	The air mass flow	*[kg/s]*
Cp	The power coefficient	
R	Resistance	*[Ω]*
V	Voltage	*[V]*
I	Current	*[A]*
A_C	the conductor area of the cable	*[m^2]*
l	the length of the cable	*[m]*
σ	the conductivity of the cable	*[S/m]*
μ_o	the magnetic constant or the permeability of the free space	*[N/A^2]*
C	the capacity of the cable	*[F]*
Qe	the electric charge stored in a conductor	*[Culomb]*
G	conductance	*[Siemens]*
γ	wave propagation constant	
α_γ	the real part of the propagation constant which represents the attenuation	*[Np/m]*
β_γ	the imaginary part of the propagation constant which represents phase velocity	*[rad/m]*
v_e	the propagation speed of the traveling wave	*[m/s]*
f_e	the frequency of the analyzed transient phenomenon	*[Hz]*
λ	The traveling wave length	*[m]*
Z	the total series impedance of the circuit	*[Ω]*
Y	the total shunt admittance of the circuit	*[Ω^{-1}]*
Z_c	The characteristic impedance	*[Ω]*
ω	the angular speed	

f	The frequency	*[Hz]*
τ	Travelling wave's time delay	*[s]*
ρ_c	the resistivity of the material	*[Ω*m]*
D	The diameter	*[m]*
μ	the absolute magnetic permeability ($\mu_0\ \mu_r$),	N/A^2
μ_r	the relative magnetic permeability	
A_s	The shield's cross section	*[m* ^{2}*]*
R_s	Outer radius of the shield	*[m]*
r_s	Inner radius of the shield	*[m]*
ε_r	The dielectric constant	
X	reactance	*[j Ω]*
Q	Reactive power	*[VAR]*
Ry	Rayleigh's probability distribution	
A	Avaiavility	*[%]*
f_{rate}	Failure rate	*[failure/year]*
lf_{years}	Life time	*[years]*
E_{trans}	Transmitted energy	*[MWh]*
$C_{platform}$	Cost of the platform	*[M€]*
$C_{transform}$	Cost of the transformer	*[M€]*
C_{comp}	Cost of the reactive power compensation	*[M€]*
C_{invest}	Investement cost	*[M€]*
C_{trans}	Transmission cost	*[M€]*

Subscripts

wind	Wind
HVAC	High Voltage AC transmission
MVAC	Medium Voltage AC transmission
cable	Cable
loss	Active power losses
active	Active
reactive	Reactive
C	Capacitor
L	Inductor
comp	Compensation
max	Maximum
min	Minimum
trafo	Transformer
repair	repair
avg	Average
sc	Short circuit
pcc	Point off common coupling
pc	Collector point
ac	Altern current
t	Total value
n	Nominal
in	Input
out	Output
loss_avg	Average active power losses
life	Usefull life time
rect	Rectifier
filter	Filter
bus	Bus
chopper	Chopper
d	Direct
q	Quadrature
shock	Shock
dip	Dip
res	Residual
TOL	Tolerance
prim	Primary
sec	Secondary
mag	Marnetization
windfarm	Windfarm
on	Onshore
off	Offshore
resonance	Resonance

Superscripts

*	Reference
+	Positive sequence
-	Negative sequence

Abbreviations

AC	Altern current
HVAC	High Voltage AC transmission
MVAC	Medium Voltage AC transmission
DC	Direct current
HVDC	High voltage direct current
EMTP	Electromagnetic transients program
LCC	Line commutated converters
VSC	Voltage source converter
MTTR	Mean Time To Repair
O & M	Operating and maintenance
XLPE	Cross Linked Polyethylene
SO	System operator
LVRT	Low voltage ride through
PCC	Point of common coupling
PC	Collector point
SCIG	Squirrel cage induction generator
WRIG	Wound rotor induction generator
PMSG	Permanent magnet synchronous generator
WRSG	Wound rotor synchronous generator
DFIG	Double fed induction generators
PWM	Pulse width modulation
THD	Total harmonic distortion
PF	Power factor
IEGT	Injection Enhanced Gate Transistor
PLL	Phase lock loop
PI	Proporcional integral
SSM	Sequence separation method
DSC	Delayed signal cancellation
NPC	Neutral point clamped
REE	Red Eléctrica Española
PVVC	Procedure to verification, validation and certification
STATCOM	Static synchronous compensator
SVC	Static Var Compensator

Appendix B: Power Factor Requirements at the Point of Common Coupling

International grid codes demand to wind farms the control of the power factor at the PCC. Moreover, some of them have as a requirement the control of this power factor depending on the voltage of the PCC.

For example, ELTRA (Denmark), ESB (Irish) and AMC (Australia) grid codes requires a minimum power factor at the PCC independently of the voltage [129], [130], [131] Figure B.1.

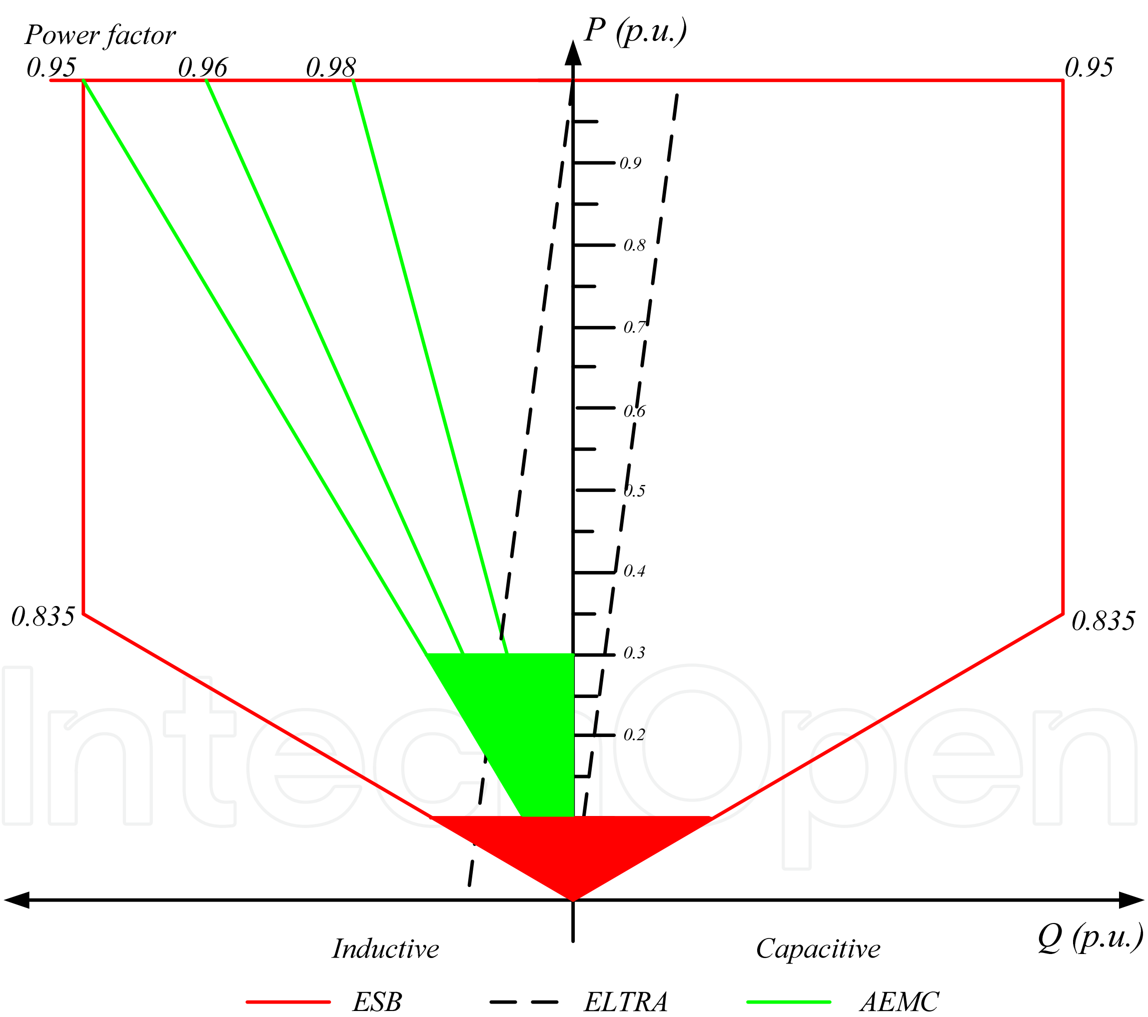

Figure B.1 Power factor requirements at the PCC for several international grid codes.

However, other grid codes: like E.ON or UK national grid, have limited the power factor depending on the voltage in order to contribute to the voltage regulation of the node [132], [89].

As an example, E.ON establishes for normal operation, the power factor boundaries depicted in Figure B.2.

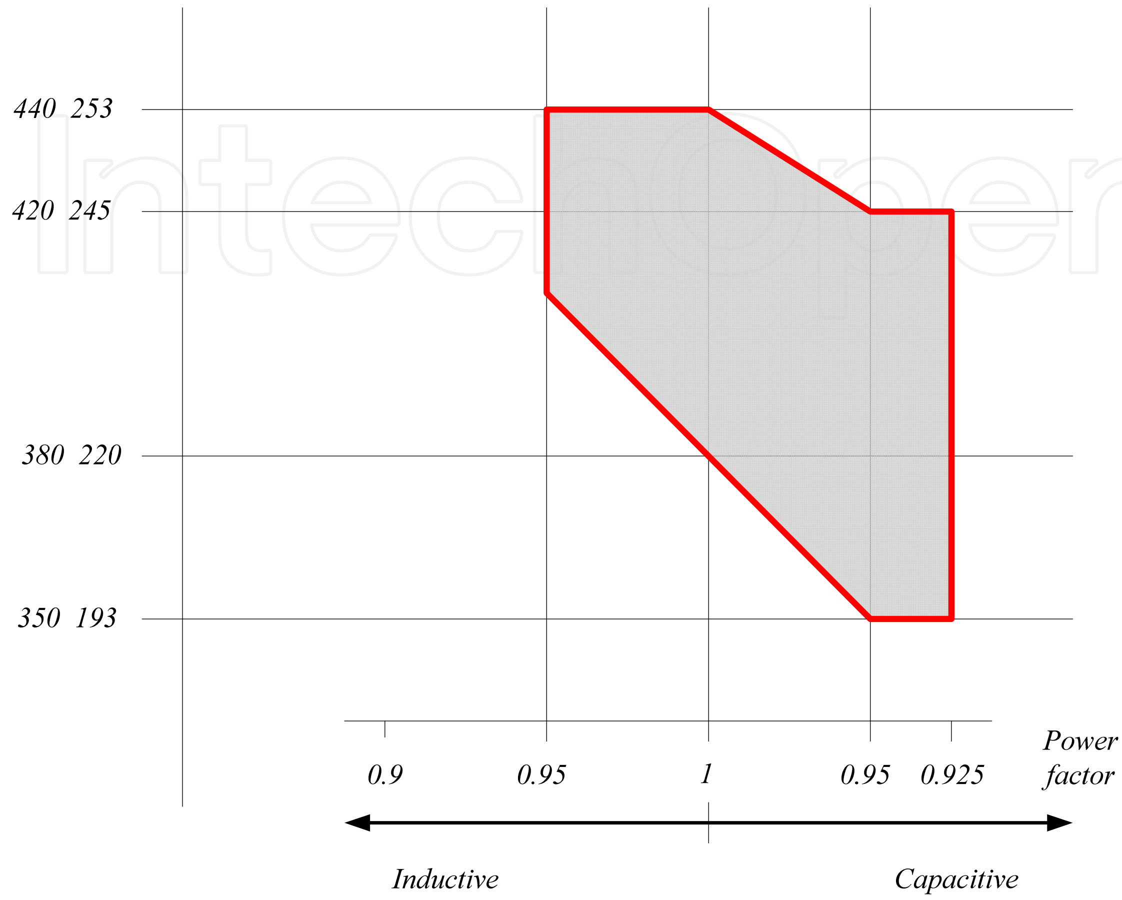

Figure B.2 Power factor requirements in the PCC depending on the voltage for E.ON.

Appendix C: REE Grid Code Requirements for Voltage Dips

The grid code requirements for voltage dips in Spain are described at the operation procedure P.O. 12.3 (requirements for voltage dips in electrical wind installations) [100] developed by REE (Red Eléctrica de España).

Summarizing the LVRT characteristics required by REE, these can be divided into two fault groups with different requirements (balanced and unbalanced faults) and two different groups of voltage dips:

- Mono phase faults, three-phase faults and two phase-to-ground.
- Two phase ungrounded faults.

In this way, REE grid code specifies that the wind farms (and all their equipments) must not be disconnected, if a three-phase, two phase-to-ground or one-phase faults with characteristics inside the voltage/time curve depicted in Figure C.1 occurs. After fault-clearing the time necessary to recover nominal values depends on the percentage of the wind generation penetration related to the short circuit power

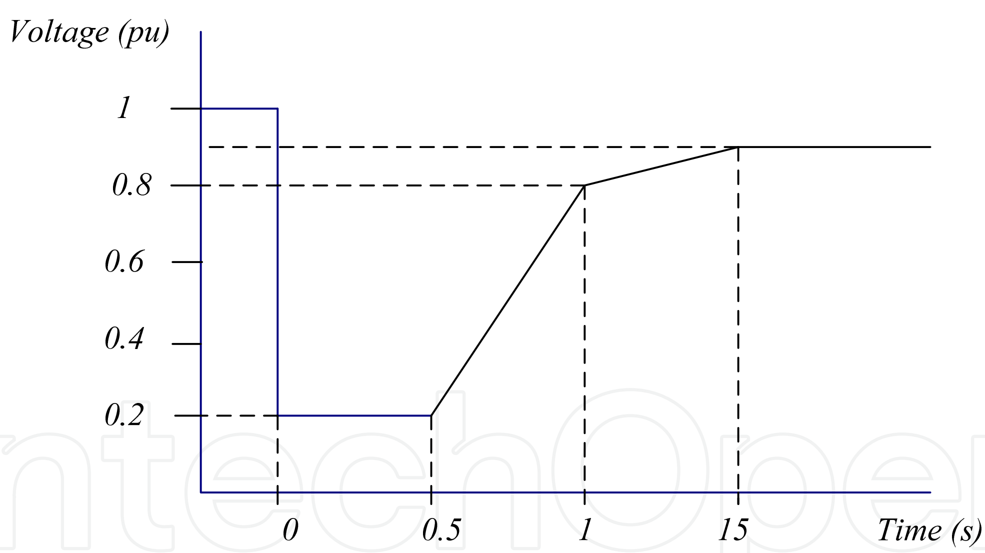

Figure C.1 Voltage / time curve admitted at the PCC for three-phase, two phase-to-ground and one-phase faults

In the case of phase-to-phase short-circuits (two phase ungrounded faults), the maximum voltage drop is 0.6 pu, instead of 0.2 pu. Thus, the wind turbines must not be disconnected if a two phase ungrounded fault with characteristics inside the voltage/time curve depicted in Figure C.2 occurs.

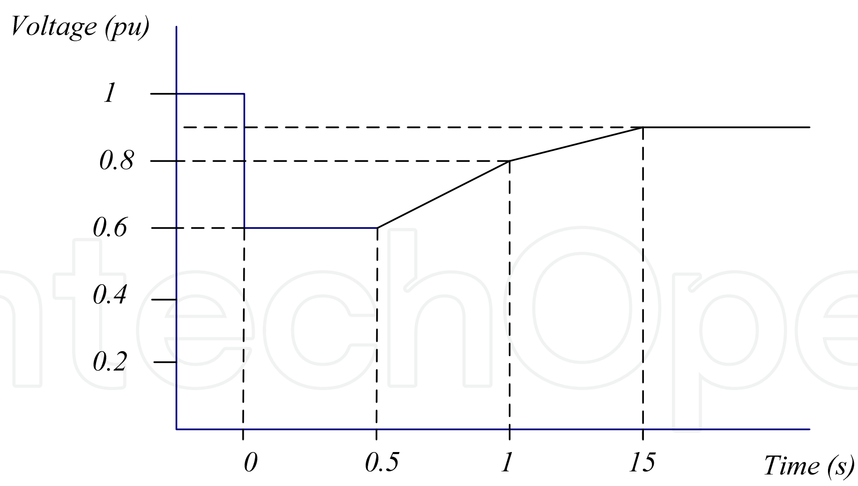

Figure C.2 Voltage / time curve admitted at the PCC for two-phase ungrounded faults

Wind farm also must provide reactive current to the grid at the PCC during the fault and later in the voltage recovery period. In any case, this current must be located in the shaded area in Figure C.3, within 150 ms after the beginning of the fault or after the clearance of the fault. Thus, the wind farm must generate reactive current with voltages below to 0.85 pu, and it must not consume reactive power between 0.85 pu and the rated voltage.

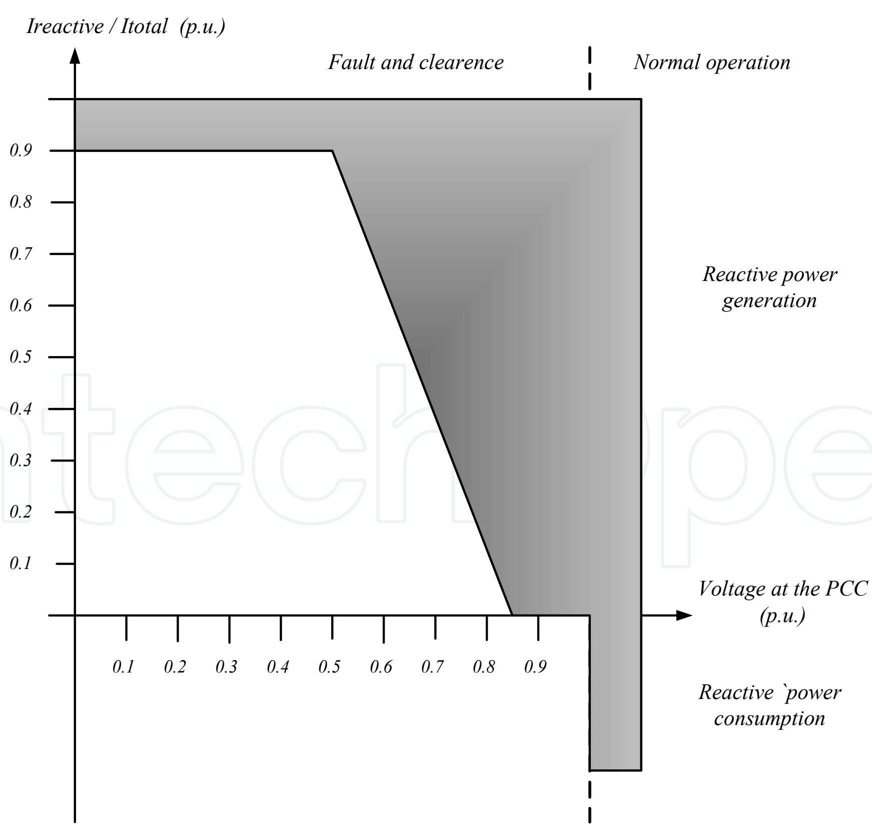

Figure C.3 Reactive current / total current requirement depending on the voltage at the PCC.

Requirements for balanced three-phase faults

Wind farms will not absorb reactive power during either balanced three-phase faults, or the voltage recovery period after the clearance of the fault. However, reactive power absorptions are allowed during a period of 150 ms after the beginning of the fault, and also 150 ms after the clearance of the fault, with two constrains:

- The net reactive power consumption of the wind farm during the 150 ms interval after the beginning of the fault, in 20 ms cycles, must not exceed 60% of its rated power.
- The net reactive energy consumption of the wind farm after the clearance of the fault must not exceed 60% of its rated power, and the reactive current, in 20 ms cycles, must not exceed 1.5 times the rated current.

With regards to the active power, the wind farm at the PCC must not absorb active power during the fault or the voltage recovery period after the clearance of the fault. However, absorption of active power is accepted for 150 ms after the beginning of the fault and also 150 ms after the clearance of the fault. During the rest of the fault, the active power consumptions are additionally allowed, but have to be less than the 10% of the wind farm rated power.

Requirements for unbalanced two-phase and single-phase faults

Wind farms will not absorb reactive power in the PCC during either unbalanced two-phase and single-phase faults, or the voltage recovery period after the clearance of the fault. Nonetheless, reactive power absorptions are allowed during a period of 150 ms after the beginning of the fault, and also 150 ms after the clearance of the fault, with two constrains:

- The net reactive power consumption of the wind farm, during the 150 ms interval after the beginning of the fault, will not exceed the 40% of its rated power during a period of 100 ms
- The net reactive power consumption of the wind farm after the fault clearance, in 20 ms cycles, will not exceed the 40% of its rated power.

Additionally, transitory consumption is admitted during the rest of the fault with two constraints:

- The net active consumption must not exceed the 45% of the equivalent rated active energy of the wind farm during a period of 100 ms.
- The consumption of active power, in cycles of 20 ms, must not exceed the 30% of its rated active power.

Appendix D: Clarke and Park Transforms

The *dq* transformation is a transformation of coordinates from a three-dimensional stationary coordinate system to the *dq* two-dimensional rotating coordinate system. This transformation is made in two steps:

- **Clarke Transformation**, a transformation from the three- dimensional stationary coordinate system to a two- dimensional, *αβ* stationary coordinate system.
- **Parke Transformation**, a transformation from the *αβ* stationary coordinate system to the *dq* two- dimensional rotating coordinate system.

Clarke Transformation, from *abc* to *αβ*

A representation of a vector in a three-dimensional space is accomplished through the product of a transpose three-dimensional vector (base) of coordinate units and a vector representation of the vector, whose elements are corresponding projections on each coordinate axis, normalized by their unit values.

If the vector has not any component (the projection on one of the three axes is zero) in one of the coordinate axis, it is possible to transform this vector into an equivalent vector in a two-dimensional space without losing information.

Therefore, if a three-phase space vector in a three-dimensional space has not any component in one of the coordinate axes, the space vector can be transformed into a two-phase space vector in a two dimensional space, in order to simplify the work with them.

Furthermore, if the phase *a* is arbitrarily chosen to coincide with *a,* the new axes of the two-phase coordinate system, the transformations is even more simple. It can be made applying the equation (150), Figure D.1.

$$X_{\alpha\beta} = X_{abc}T = X_{abc}\frac{2}{3}\begin{bmatrix} 1 & 0 \\ -\frac{1}{2} & \frac{\sqrt{3}}{2} \\ -\frac{1}{2} & \frac{\sqrt{3}}{2} \end{bmatrix} \tag{150}$$

$$X_{abc} = \begin{bmatrix} a_u & b_u & c_u \end{bmatrix} \tag{151}$$

$$X_{\alpha\beta} = \begin{bmatrix} \alpha_u & \beta_u \end{bmatrix} \tag{152}$$

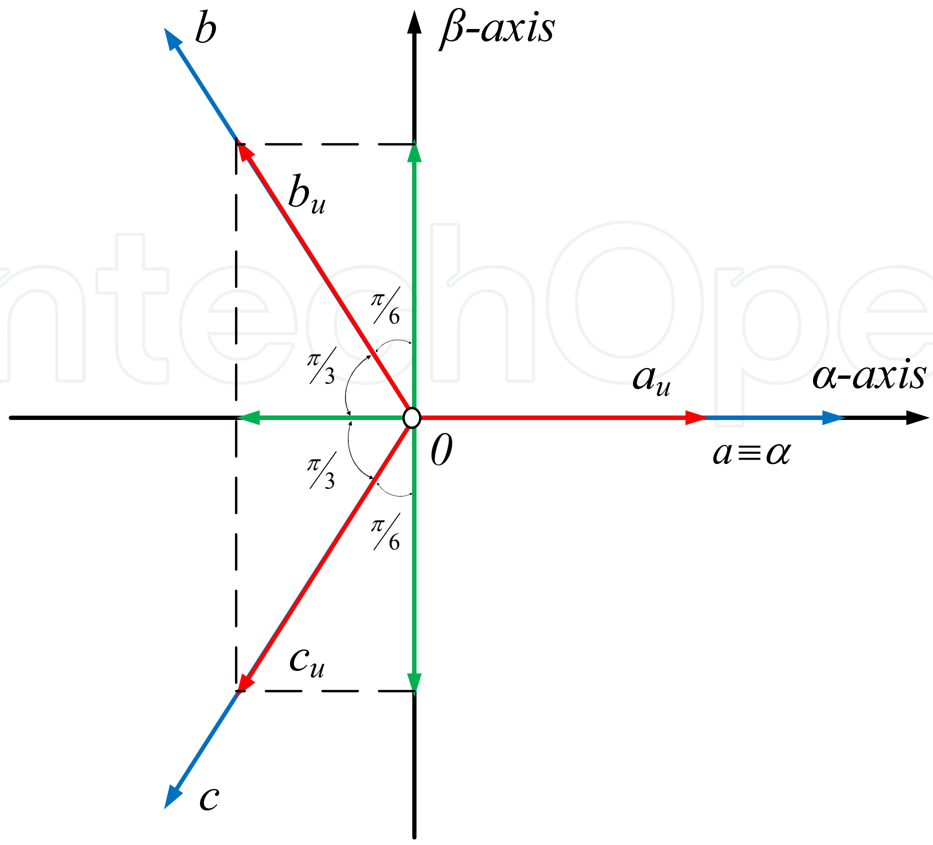

Figure D.1 Vector representation of the *abc* to *αβ* transform.

Without assuming that the three-phase space vector in the three-dimensional space has not any projection on one of the three axes ($0_u \neq 0$), the three-phase space vector representation transforms to *αβ* vector representation through the transformation matrix defined as:

$$X_{\alpha\beta 0} = X_{abc}\,\frac{2}{3}\begin{bmatrix} 1 & 0 & \frac{1}{2} \\ -\frac{1}{2} & \frac{\sqrt{3}}{2} & \frac{1}{2} \\ -\frac{1}{2} & \frac{\sqrt{3}}{2} & \frac{1}{2} \end{bmatrix} \tag{153}$$

$$X_{\alpha\beta 0} = \begin{bmatrix} \alpha_u & \beta_u & 0_u \end{bmatrix} \tag{154}$$

Parke Transformation, *αβ* to *dq*

For the last step, the *αβ* stationary coordinate system is transformed to the *dq* two-phase rotating coordinate system, equation (155), Figure D.2. This last transformation simplifies the work with rotational three-phase space vectors, due to the fact that if the quadrature axes and the space vector ($X_{\alpha\beta}$) are rotating at the same speed ωt, from the rotating point of view of the quadrature axes, the space vector is stationary.

$$X_{dq0} = X_{\alpha\beta 0}\begin{bmatrix} \cos\theta & -\sin\theta & 0 \\ \sin\theta & \cos\theta & 0 \\ 0 & 0 & 1 \end{bmatrix} \tag{155}$$

$$X_{dq0} = \begin{bmatrix} d_u & q_u & 0_u \end{bmatrix} \tag{156}$$

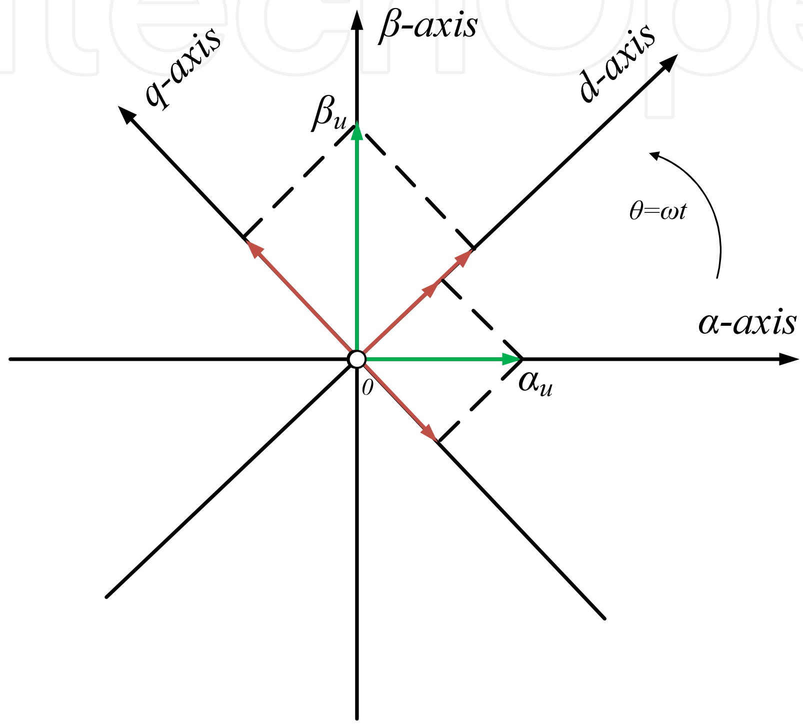

Figure D.2 Vector representation of the *αβ* to *dq* transform.

For the direct transformation, a three-phase vector representation transforms to *dq* vector representation through the transformation matrix *T*, defined as:

$$X_{dq0} = X_{abc}T = X_{abc}\,\frac{2}{3}\begin{bmatrix} \cos\theta & \sin\theta & 1/2 \\ \cos\left(\theta - 2\pi/3\right) & \sin\left(\theta - 2\pi/3\right) & 1/2 \\ \cos\left(\theta + 2\pi/3\right) & \sin\left(\theta + 2\pi/3\right) & 1/2 \end{bmatrix} \tag{157}$$

And the inverse transformation is:

$$X_{abc} = X_{dq0}T^{'} = X_{dq0}\begin{bmatrix} \cos\theta & \cos\left(\theta - 2\pi/3\right) & \cos\left(\theta + 2\pi/3\right) \\ \sin\theta & \sin\left(\theta - 2\pi/3\right) & \sin\left(\theta + 2\pi/3\right) \\ 1 & 1 & 1 \end{bmatrix} \quad (158)$$

Appendix E: Resonant Passive Filters

The resonant passive filters are constituted by a capacitor, a inductor and a resistor, there are basically electrical branches (RLC branches).

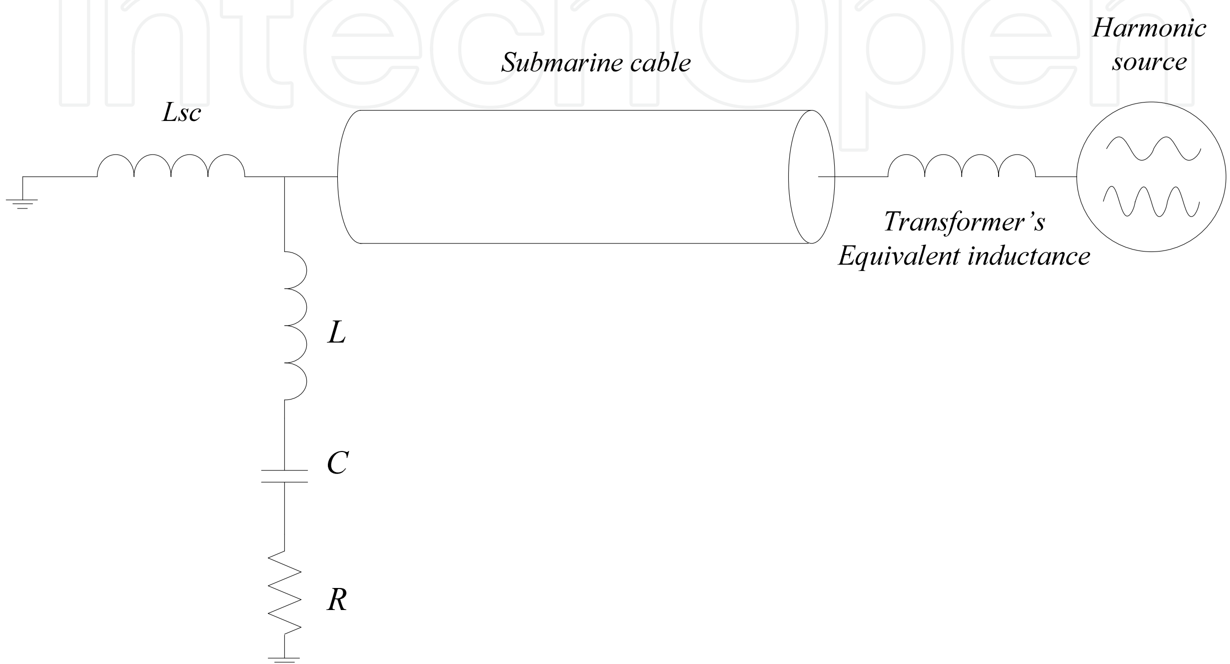

Figure E.1 The transmission system with a RLC filter.

The main characteristic of a RLC branch is the delay of 180º between the voltage dropped in the inductive impedance and the voltage dropped in the capacitive impedance. As a result, in a specific frequency, the electric branch only presents the resistive impedance.

The resonant passive filters are based on this characteristic to filter a specific harmonic. The RLC branch is tuned to presents only the resistive part at the frequency where is located the harmonic. So, at this specific frequency, the RLC branch presents very low impedance and absorbs the harmonic current.

In this way, the harmonic current generated in a device or devices is deviated to the filter instead to flow to the distribution grid or power source. More specifically, the generated harmonic current goes to the grid and to the RLC filter, where the harmonic current is divided depending on kirchoff's law, in the inverse proportion of the impedances. Thus, the filter absorbs more or less of the harmonic current depending on the system impedance and the impedance of the filter at this specific frequency, Figure E.2.

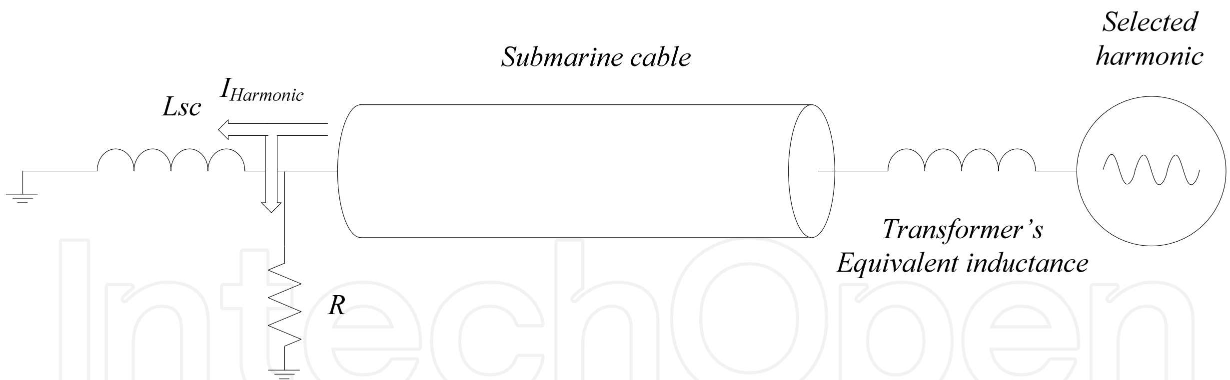

Figure E.2 Transmission system with a RLC filter at the resonance frequency of the filter.

The harmonic current flows through the part of system between the source and the RLC filter. The harmonic current, generates harmonic voltages between the source and the filter, and this harmonic provokes the disturbances described in section 6.2, but the objective of this filter is the reduction of the harmonics waters down the RLC filter. For instance, the reduction of the harmonic levels at the PCC.

Highlight that to achieve a reduction bigger than the 50% of any harmonic current with this kind of filters (a RLC branch in parallel with the circuit), the impedance of the filter at the selected frequency have to be less than the impedance presented by the circuit at this frequency.

RLC impedance depending on the frequency

To carry out the evaluation of the impedance, current and voltage through the RLC branch depending on the frequency, there is considered the generic RLC filter depicted in Figure E.3

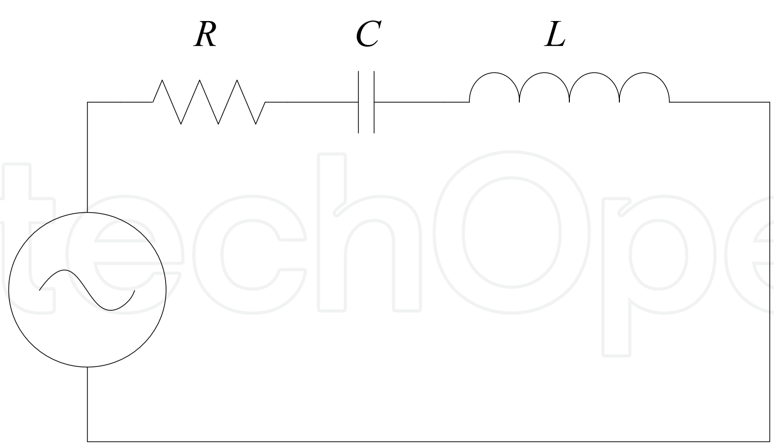

Figure E.3 Generic RLC circuit.

Looking at Figure E.4, the diagram of the RLC branch voltages shows a voltage drop in phase with the current in the resistance, a voltage drop delayed 90º with the current in the capacitor and a voltage drop (delayed -90º) 90º forward the current in the inductor.

The voltage dropped in the capacitor has a difference of 180º with regard to the voltage dropped in the inductor, so, the both voltages are counteracting each other. Consequently, the reactive voltage vector of the RLC branch is the subtraction of these two vectors V_{XL} – V_{XC} (or V_{XC} – V_{XL}).

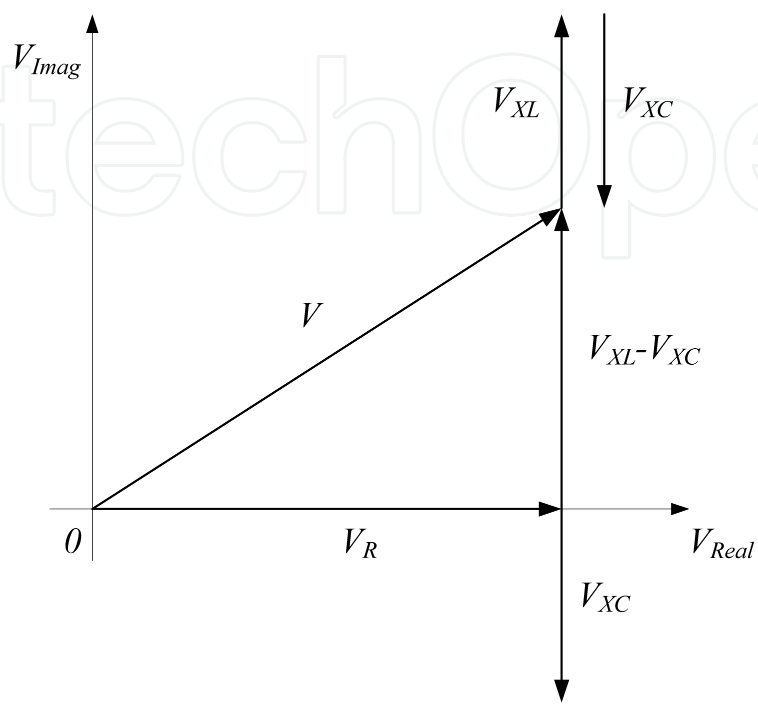

Figure E.4 Diagram of the voltages of the RLC branch.

Therefore, the total impedance of the RLC branch in complex form can be calculated via equation (159).

$$Z = R + \left(jX_L - jX_C \right) \quad (159)$$

Resonance

A circuit is (or goes to) in resonance when the applied voltage and the current through the circuit are in phase. Thus, it is possible to conclude that in resonance, the total impedance of the circuit is equal to its resistive part, i.e. the reactive impedance of the capacitor and the reactive impedance of the inductor are the same, but delayed 180º.

In short, in resonance, the reactive part of the circuit impedance has to be zero. This occurs for a specific frequency value and this frequency is the so called resonance frequency. In the RLC circuit, there are two independent parameters: *L* and *C*. Thus, there are infinite combinations to obtain a resonance in any specific frequency.

At Figure E.5, the impedance of each component of the electric branch (inductive, capacitive and resistive) depending on the frequency is represented.

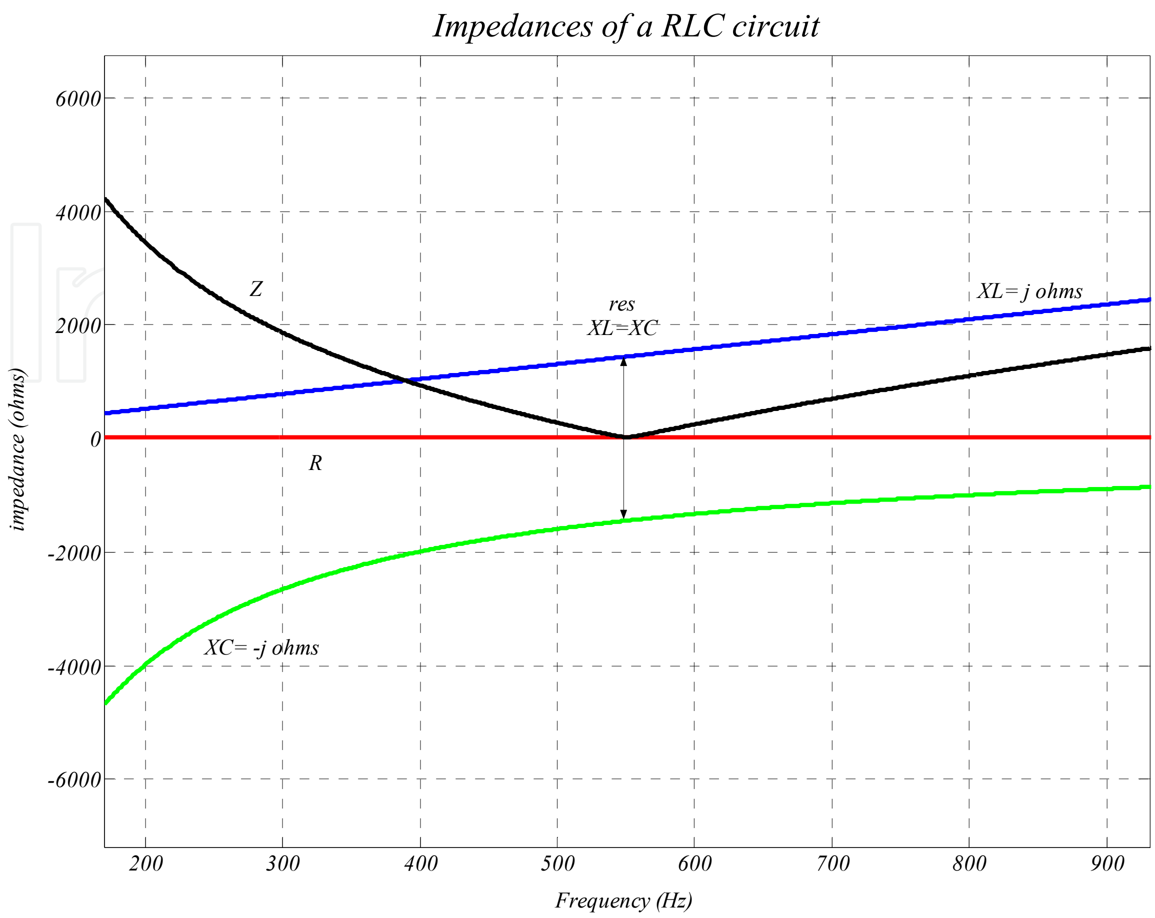

Figure E.5 Impedance of each component of the RLC branch depending on the frequency.

As can be seen in Figure E.5, the resistive part of the total impedance (*R*) is constant, i.e. it is not frequency dependent. However, the inductive part of the total impedance (*ZL*) grows up linearly with the frequency and the capacitive part (*ZC*) grows up exponentially with the frequency from "minus infinite" (for zero Hz) to zero (for an infinite value of frequency).

So, the total impedance of the branch (*Z*) decreases to the value of the resistive component (at the resonance frequency) and then grows up again. Thus, the resistance is the impedance which limits the current when the circuit is in resonance.

To characterize in more detail this relation between the resistive component and the resonance, the admittance (*Y* = *1/Z*) of the RLC branch depending on the frequency for different R values is depicted in Figure E.6.

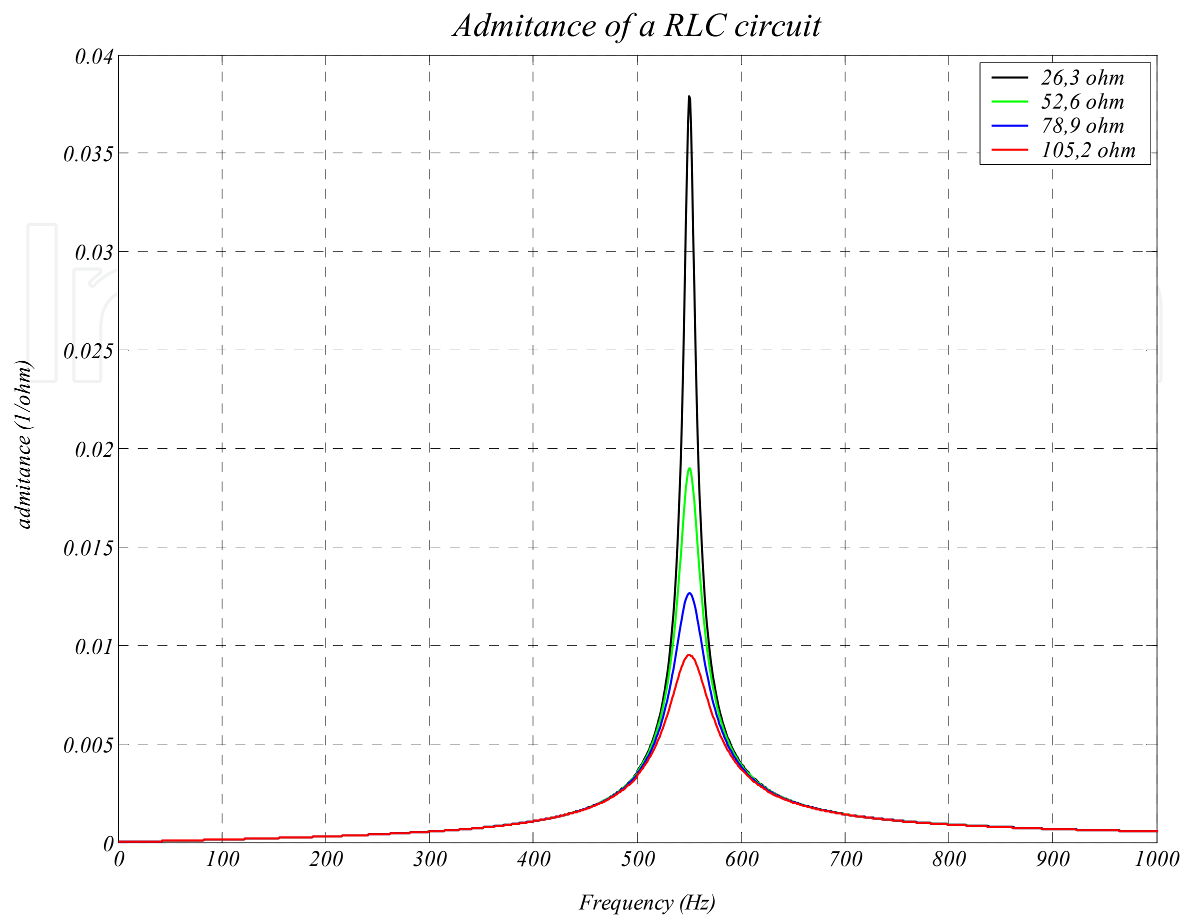

Figure E.6 The admittance of the RLC branch depending on the frequency for several values of the resistive part.

In Figure E.6, it is possible to observe that the relation between the amplitude of the resonance and the amplitude of the resistance is inversely proportional, i.e. if the smaller is the resistive part, the RLC branch can accept more current at this frequency.

Quality factor

Is called the quality coefficient or quality factor to the product of the pulsation and the relation between the maximum stored energy and the average dissipated power. This quality factor is labeled as Q and its expression is as follows:

$$Q = \frac{fo}{\Delta f} = \frac{1}{Rf} \cdot \sqrt{\frac{Lf}{Cf}} \tag{160}$$

Where: Δf is the band width.

In the same way, Q is defined as the relation between the voltage drop in the coil (or the capacitor) and the resistor. Usually, this factor has values above to 10. It is possible to see in Figure E.6, how the quality of a circuit is bigger as smaller is the resistor.

Criterions for the RLC passive filter design

To characterize adequately the resonant passive filters, there are must be taken into consideration the following aspects:

1. Power losses at fundamental frequency.
2.-Reactive power generated at fundamental frequency.
3.-The quality factor (*Q*) and the band width (Δf).
4.-Resonance frequency of the filter.
5.-The maximum harmonic voltage and harmonic current capable to support the filter, i.e. the nominal voltage and current for different components of the filter.

Notice that all of these aspects are inter related.

Active power losses mitigation

As is mentioned, resonant passive power filters have active power losses at fundamental frequency. These losses are continuous and can be significantly high. One option to reduce significantly these losses is placing an inductance in parallel with the resistor, Figure E.**7**.

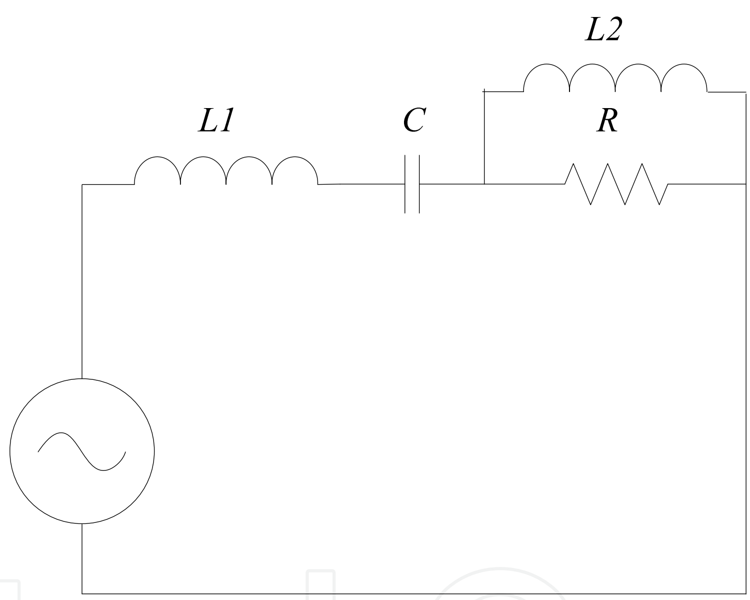

Figure E.7 Generic (R+L)LC circuit.

This inductance (L2) has to be dimensioned to present a small impedance at fundamental frequency (R>>XL2) and to present a high impedance (XL2>>R) at resonance frequency, Figure E.8.

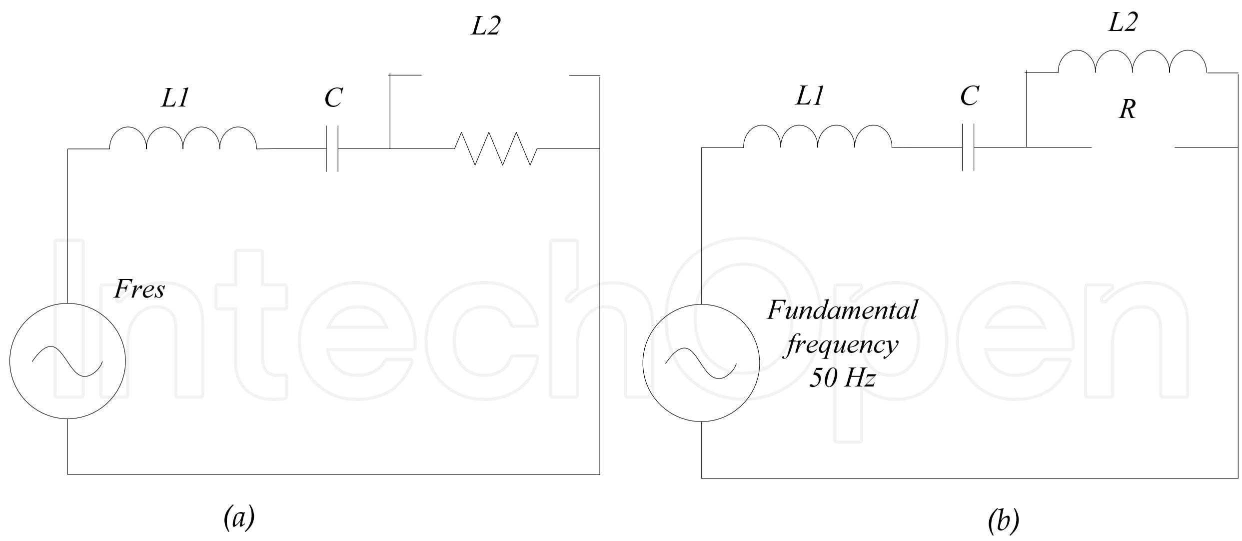

Figure E.8 Equivalent (R+L)LC circuit approximation depending on the frequency, (a) At resonance frequency and (b) at fundamental frequency.

The equivalent circuits represented in Figure E.8, shows the philosophy of this method to reduce the active power losses of the filter. Nevertheless, this representation is an approximation. Depending on the resonant frequency, this approximation will be more accurate or less.

If the resonant frequency of the branch is significantly high in comparison with the fundamental frequency (f_{res}>>$f_{fundamental}$), the difference between the impedance presented by the inductance (L2) at the fundamental frequency and at the resonant frequency is also significantly big. Thus, in this cases is possible to adjust the inductance L2 to be small at fundamental frequency and big at resonant frequency.

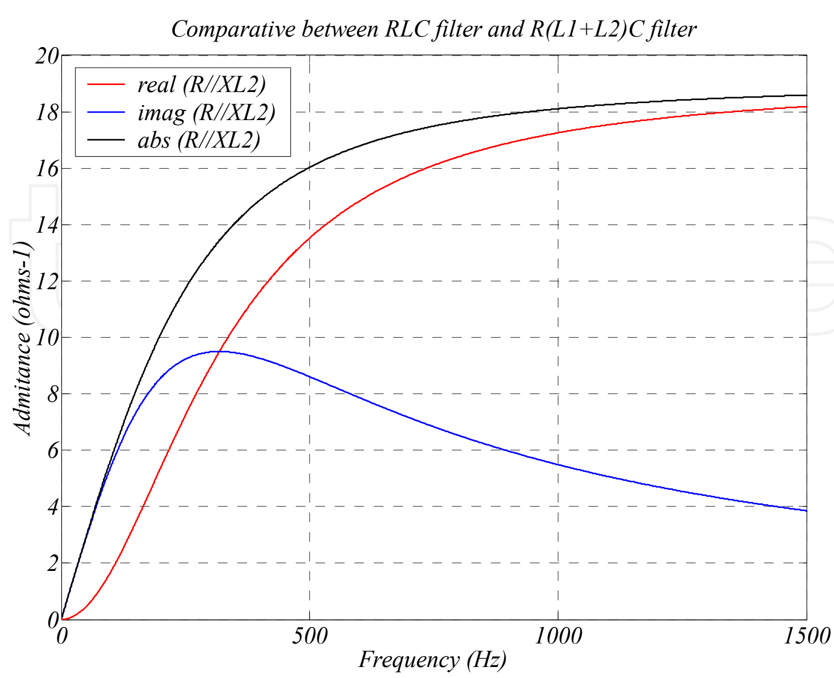

Figure E.9 Evolution of the (R+L2) impedance depending on the frequency.

The evolution depending on the frequency for the equivalent impedance presented by the inductance and the resistor (R+L2) is illustrated in Figure E.9.

Looking at Figure E.9, at low frequencies, the absolute impedance is clearly inductive (high influence of the inductance) which reduces the active power losses. However, at high frequencies, the absolute impedance is almost the same of the real value (high influence of the resistor), allowing the resistor limiting the maximum current through the branch at resonance frequency.

The new resonance frequency

As can be seen in Figure E.9, at high frequencies, the absolute impedance is almost the same of the real value, but there is still an inductive part. Therefore, this inductive component varies (reducing) the resonant frequency of the branch, Figure E.10.

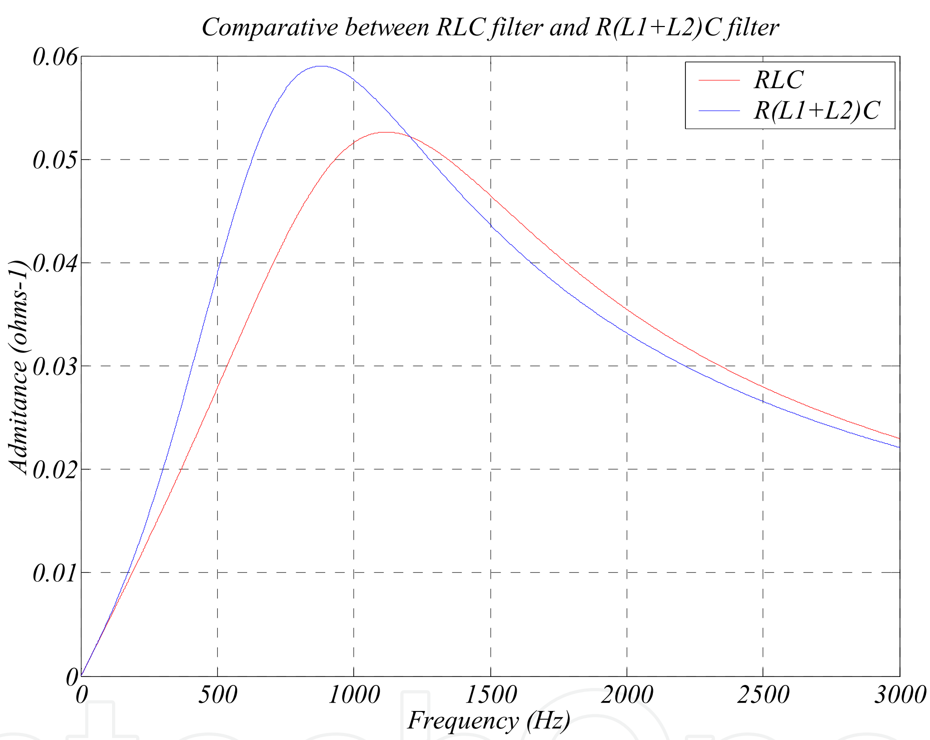

Figure E.10 Evolution of the admittance depending on the frequency. (Red) for the RLC branch and (b) for the (R+L)LC branch.

The new resonance frequency can be estimated in the same way as did for the RLC branch, due to the fact that the resonance occurs at the frequency where the inductive impedance is exactly the same of the capacitive impedance.

The only difference of this case comparing with the previous case is that the inductive impedance of the branch is given by the sum of the L1 inductance and the inductive part of the (R+L2) impedance, Figure E.11.

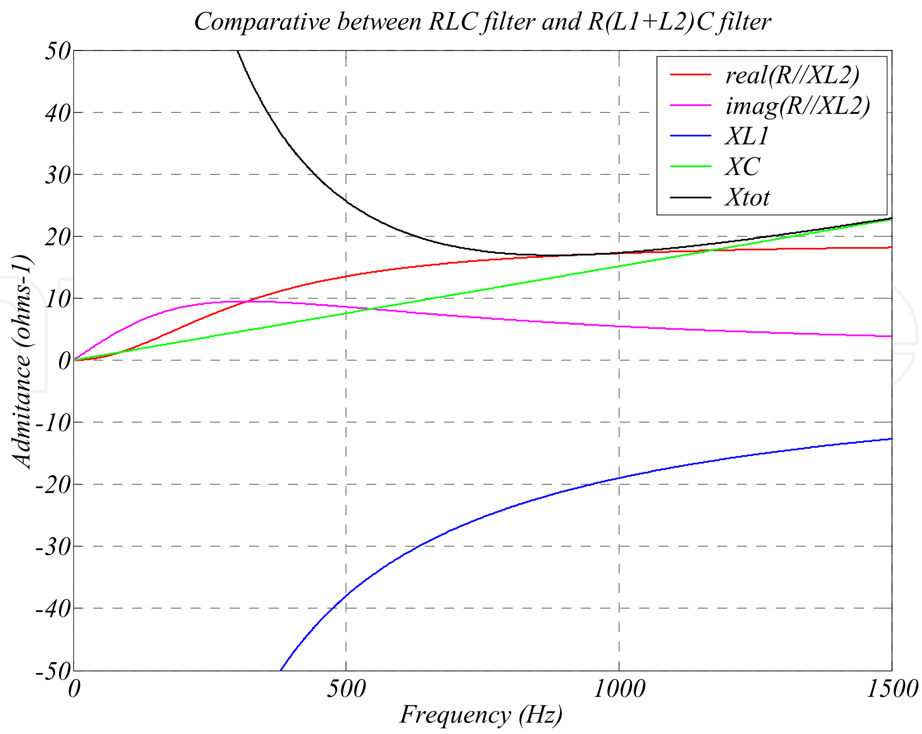

Figure E.11 Impedance of the (R+L)LC branch depending on the frequency and for each component.

Therefore, varying (reducing) the impedance of (L1) it is possible to keep the resonance frequency of the (R+L)LC at the same frequency of the RLC branch. The new value for L1 is given by the subtraction of the inductive component of the (R+L2) impedance at the resonance frequency to the impedance of the capacitor, equations (161) - (163).

$$Z_{equi} = \frac{R + jX_{L2}}{jRX_{L2}} + \tag{161}$$

$$jX_{L1}(f_{res}) = jX_C(f_{res}) - imag(Z_{equi}(f_{res})) \tag{162}$$

$$L1 = \frac{X_{L1}}{2\pi f_{res}} \tag{163}$$

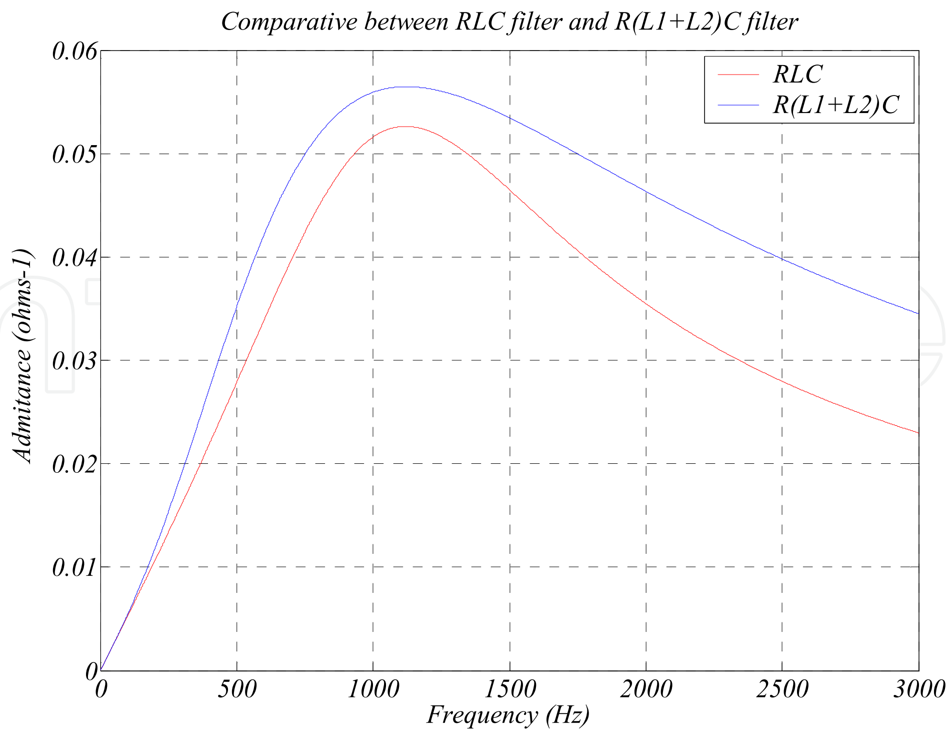

Figure E.12 Evolution of the admittance depending on the frequency. (Red) for the RLC branch and (b) for the equivalent (R+L)LC branch.

As can be seen from Figure E.12, the (R+L)LC branch has a different admittance evolution in comparison with the evolution of the RLC branch, the (R+L)LC branch has bigger band width.

Therefore, as is mentioned, this method is more appropriate for filters tuned for high resonance frequencies, the higher is the resonance frequency in comparison with the fundamental, the more similar is the evolution of the impedance of the (R+L)LC branch for the RLC branch.

Appendix F: Comparison and Validation of the Equivalent Feeder

The objective of the present appendix is to validate the simplification carried out to define the considered scenario for the problem assessment in chapter 7, section 7.2. Thus, in order to validate the simplification, a comparative between the equivalent wind turbine and the full feeder (feeder composed by six wind turbine models explained in chapter 5, section 5.2.2) is performed. In this way, it is possible to compare the behavior of these two systems and corroborate that the equivalent wind turbine exhibits a reasonably similar behavior.

For this purpose, the simulation results of the two scenarios depicted in Figure F.1 upon three-phase (80% of depth) and two-phase (40% of depth) faults are compared.

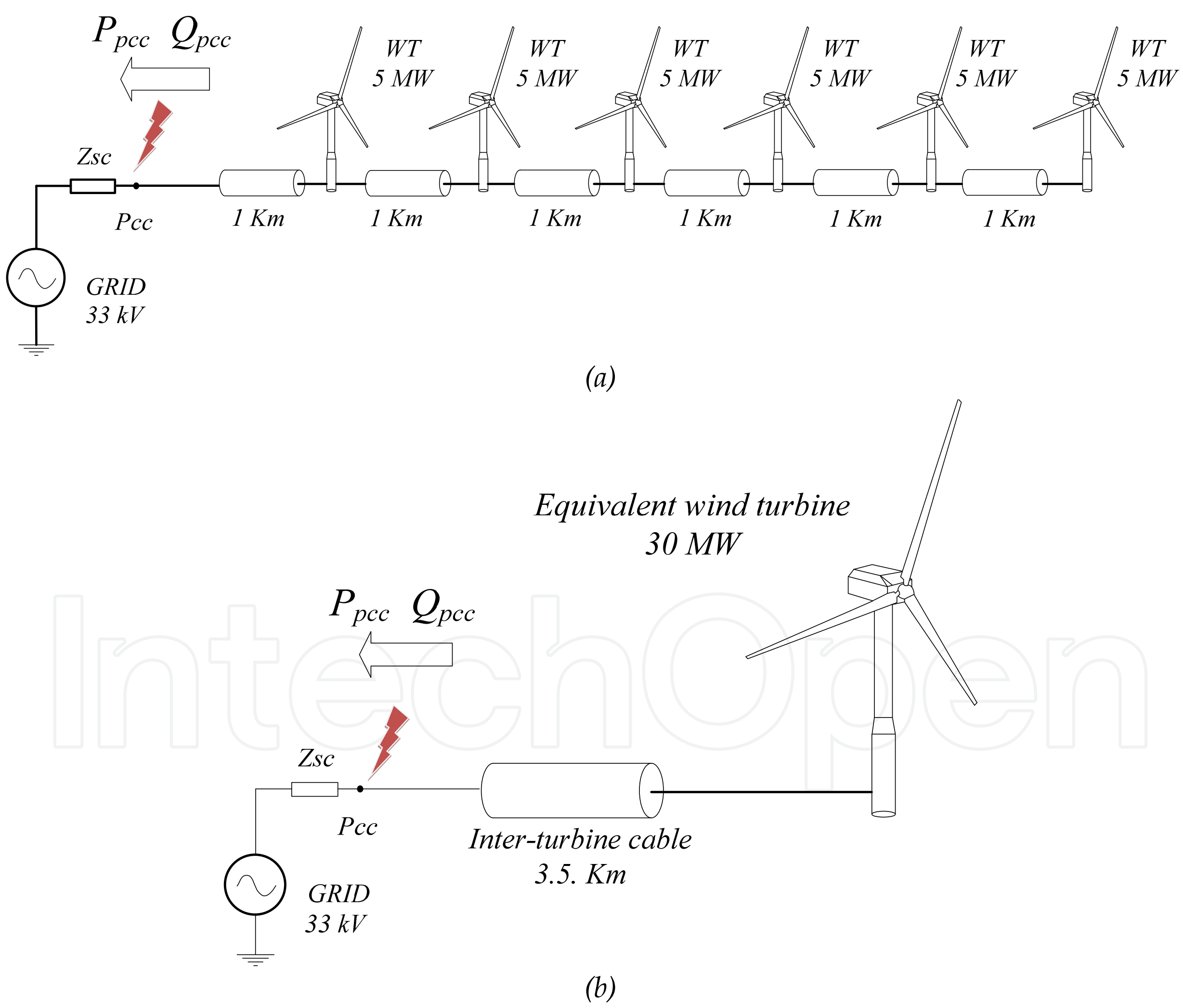

Figure F.1 Considered simulation scenarios to validate the simplification. (a) Full feeder and (b) equivalent wind turbine.

In the first step, the simulation of a three-phase fault at the PCC for both scenarios is carried out.

All the wind turbines are working at full load (90% of the nominal power, Table 5.13) and a power factor of 0.95 inductive at the PCC. The simulation results for this first case are shown in Figure F.2 - Figure F.6.

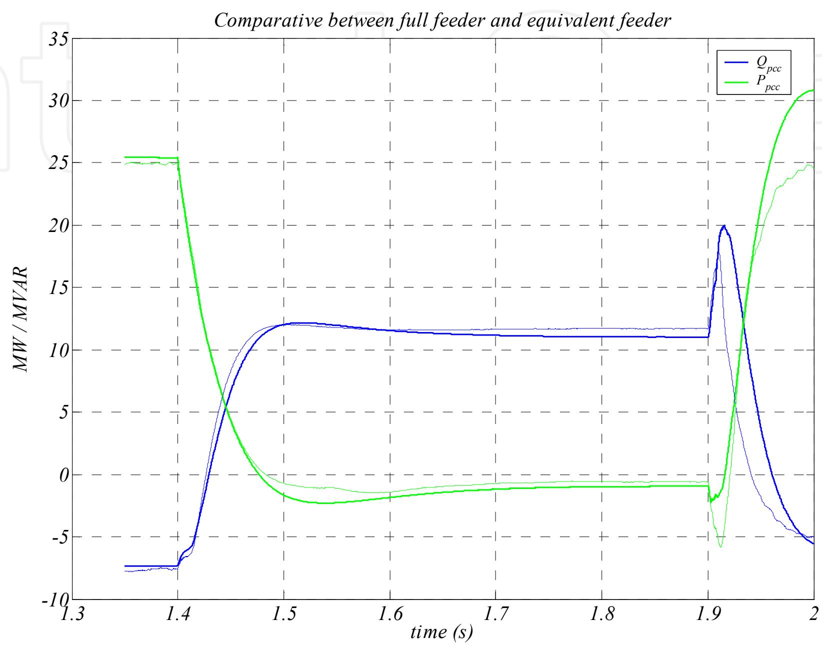

Figure F.2 Comparison of the equivalent wind turbine and the full feeder for a three-phase fault, the evolution of the active and reactive power during the fault at the PCC,

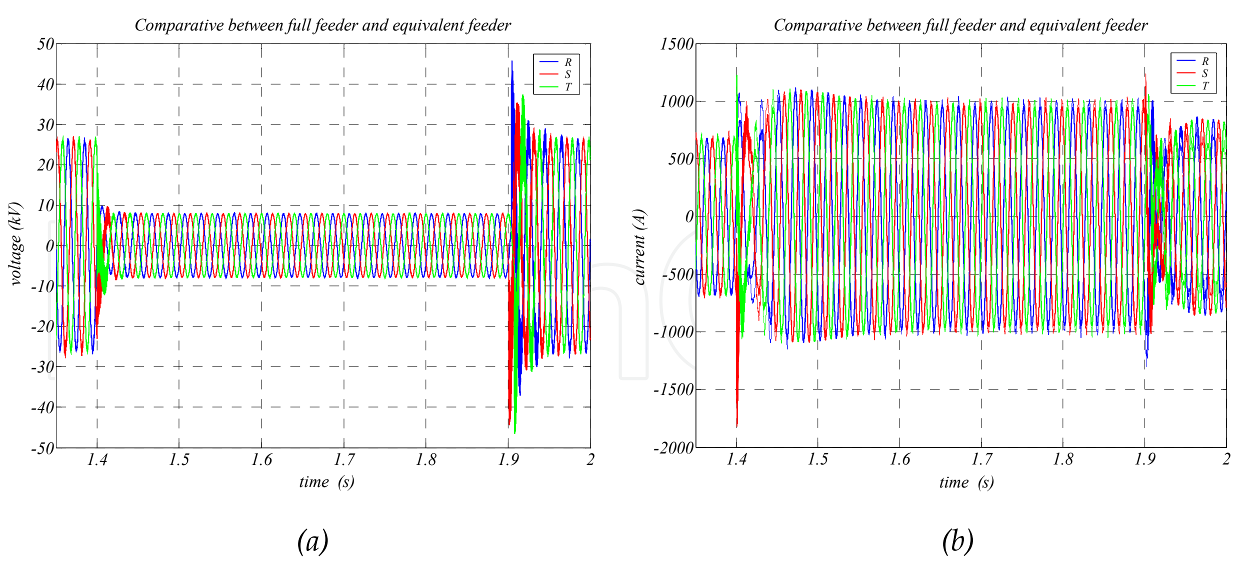

Figure F.3 Comparison of the equivalent wind turbine and the full feeder for a three-phase fault, the evolution of the voltage (a) and current (b) during the fault and the clearance at the PCC.

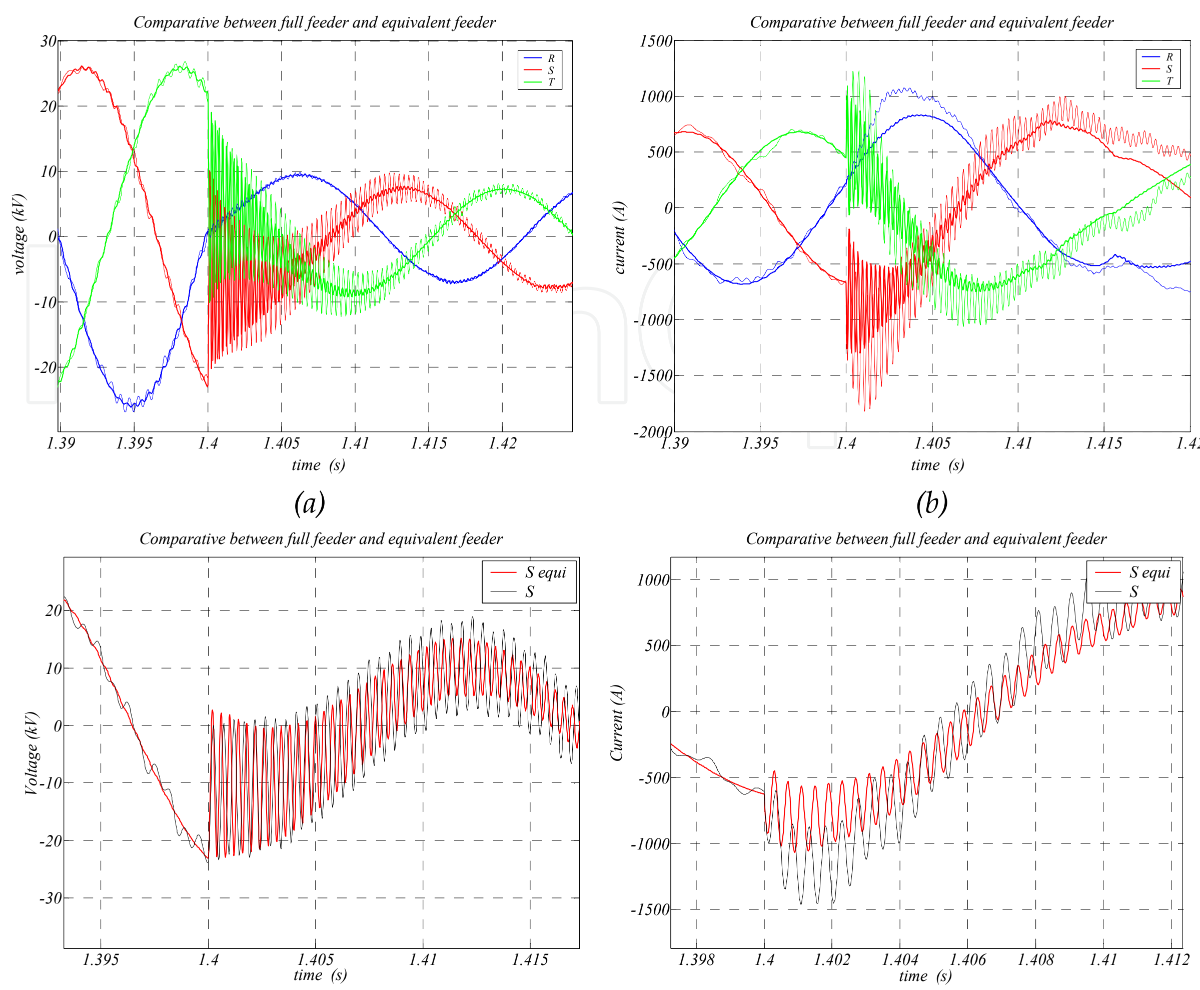

(a) (b)

(c) (d)

Figure F.4 Comparison of the equivalent wind turbine and the full feeder for a three-phase fault, the voltage (a) and current (b) at the PCC the same instant that the fault occurs, (c)-(d) at the same instant of the fault mono-phase and more detailed (red, equivalent feeder).

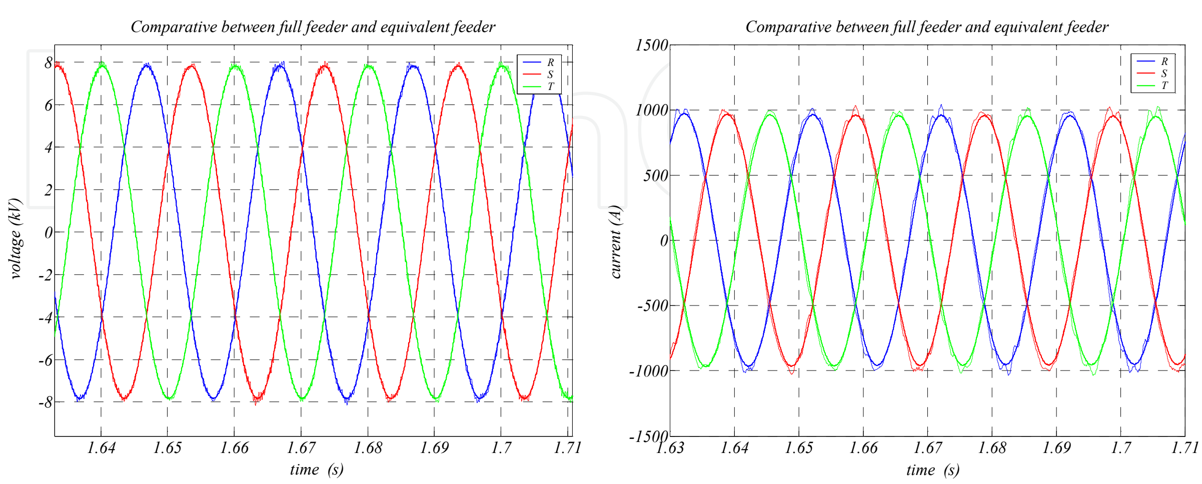

(a) (b)

Figure F.5 Comparison of the equivalent wind turbine and the full feeder for a three-phase fault, the voltage (a) and current (b) at the PCC during the maintenance of the fault.

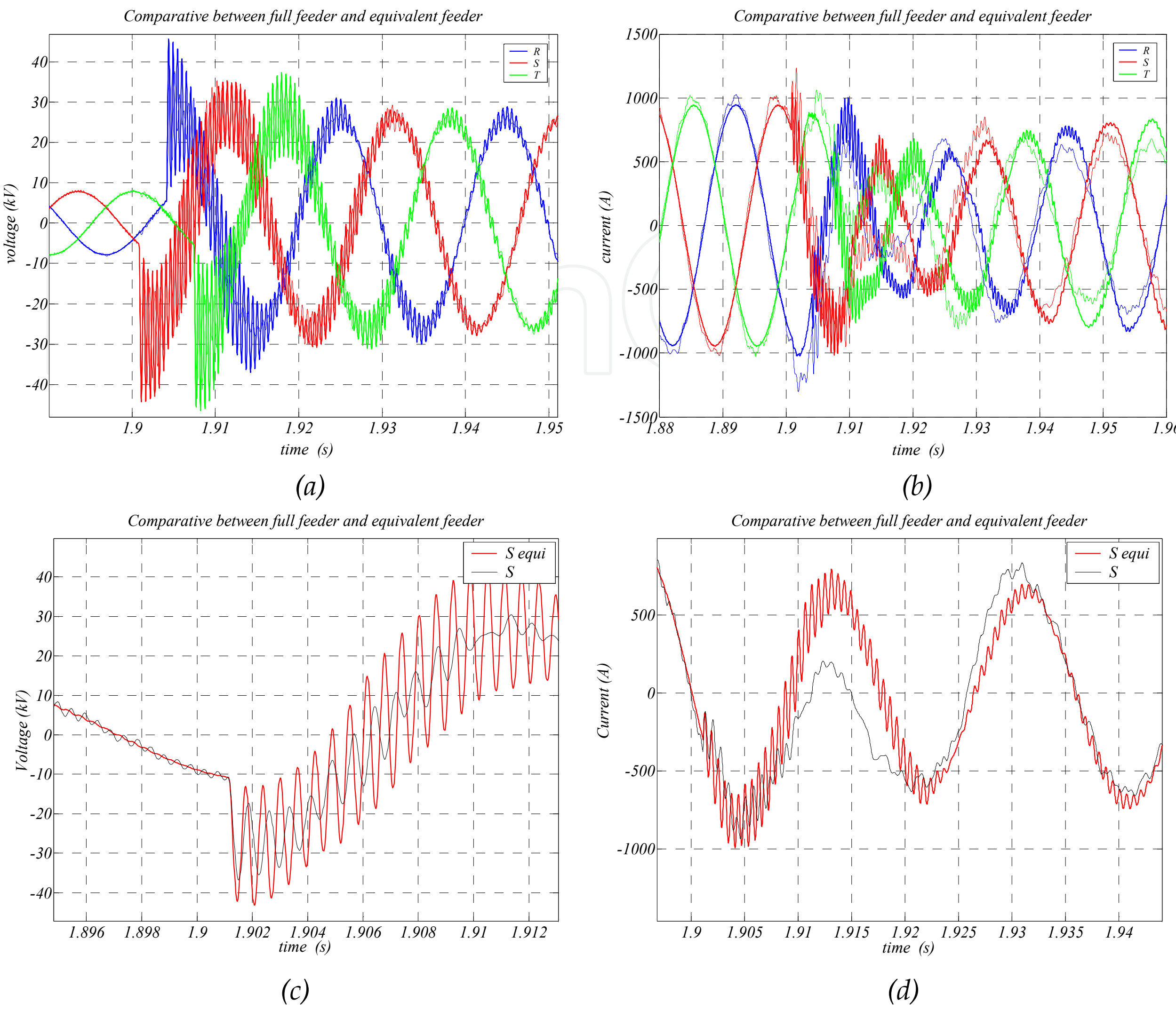

Figure F.6 Comparison of the equivalent wind turbine and the full feeder for a three-phase fault, the voltage (a) and current (b) at the PCC when the clearance of the fault occurs. (c)-(d) the voltage and current at the clearance of the fault mono-phase and more detailed, (red, equivalent feeder).

The submarine cable is simplified to generate the same reactive power, the same voltage drop and the same active power loses (equation (144)). Consequently, the results depicted in Figure F.2 are very similar.

Current and voltage peaks during the transient are caused by the energizing and de-energizing of the cable (see section 7.1). The equivalent feeder has less capacitive component and less resistive part but the same short circuit impedance. As a result, the equivalent feeder has smaller inrush current peak at the beginning of the fault (the de-energizing). The less is the capacitive component, the less is the stored energy and as a consequence needs less current for de-energizing.

Due to the fact that needs less inrush current, it is possible to see fewer low frequency oscillations before the system reaches the steady-state in the results of the equivalent feeder.

The clearance of the fault is at zero current and both the equivalent and the full feeder are connected to the grid with the same short circuit inductance, thus, both systems have the same energy stored at the magnetic field of this inductance. Therefore, the inductance transferred the same energy from the magnetic field to the electric field to adapt to the new steady-state. But, the equivalent feeder has less resistive component and less capacitive component (needs less energy to be energized). So, in contrast to the beginning of the fault, at the clearance of the fault the equivalent wind turbine has more low frequency oscillations.

Therefore, the way that is simplified the submarine cable, which varies the cable length (capacitive component of the cable), explains the difference in both transients.

Nevertheless, in steady-state the voltage and the current of the equivalent feeder have less high frequency oscillations, because is modeled with an ideal voltage source.

In the second step, the simulation of the two-phase fault is performed. The results for the equivalent wind turbine and the full feeder for this second case are depicted in Figure F.7 - Figure F.11.

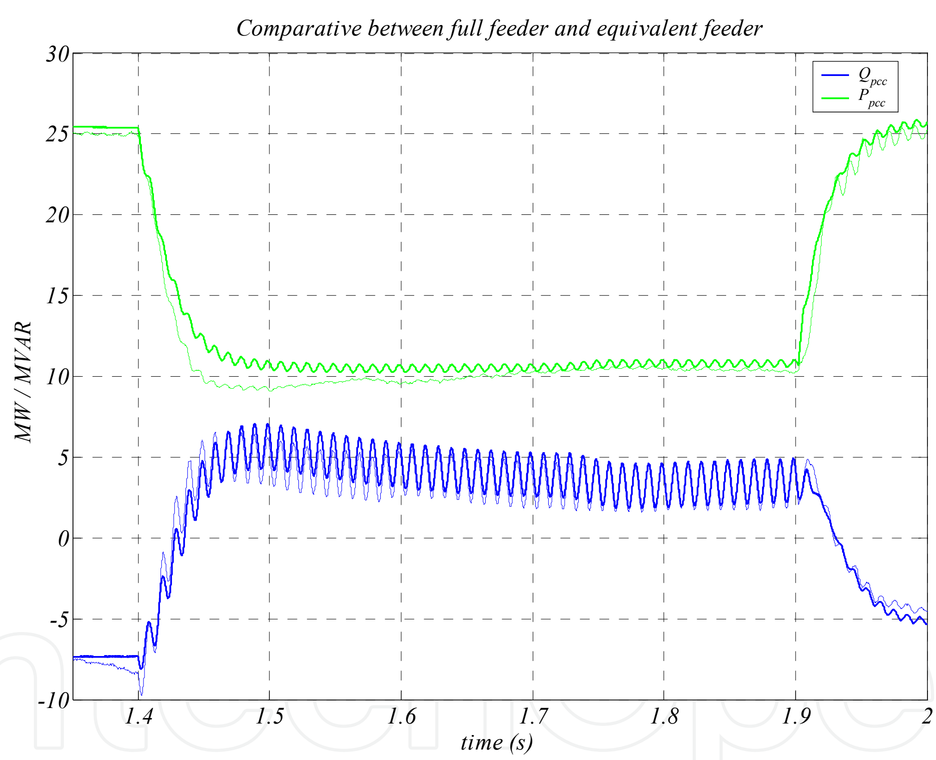

(a)

Figure F.7 Comparison of the equivalent wind turbine and the full feeder for a two-phase fault, the evolution of the active and reactive power during the fault at the PCC.

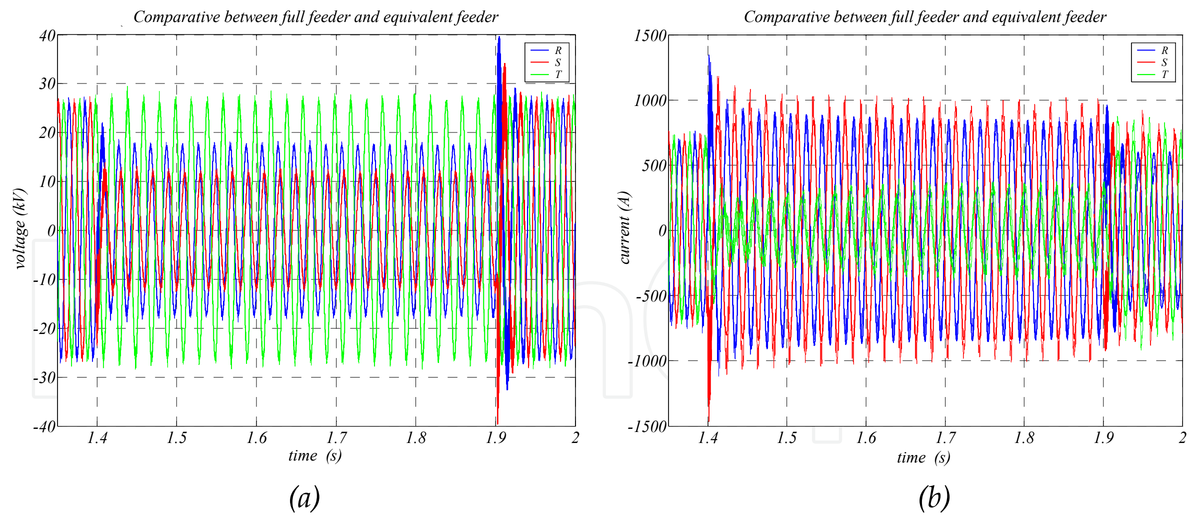

Figure F.8 Comparison of the equivalent wind turbine and the full feeder for a two-phase fault, the evolution of the voltage (a) and current (b) at the PCC during the fault and the clearance.

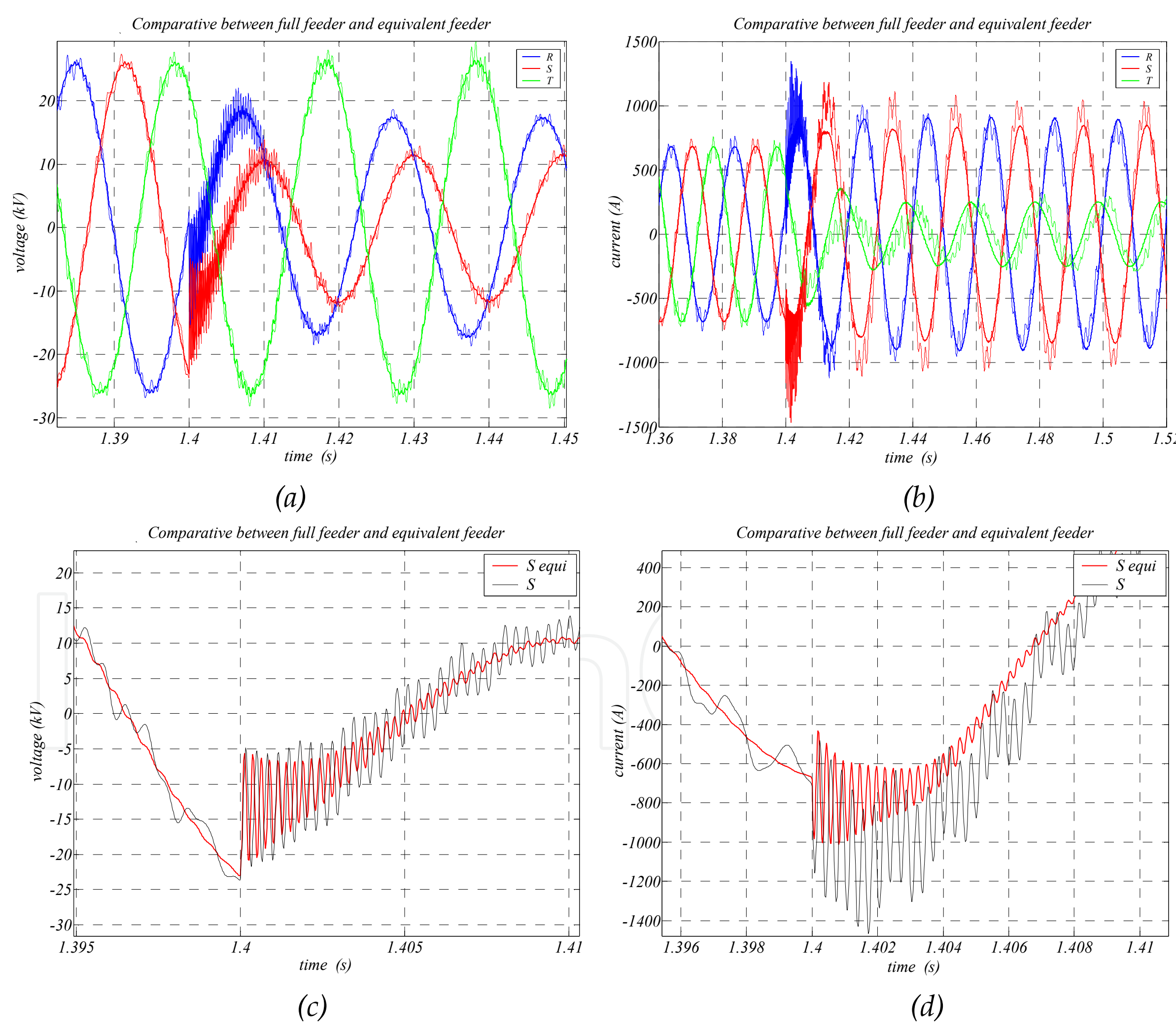

Figure F.9 Comparison of the equivalent wind turbine and the full feeder for a two-phase fault. the voltage (a) and current (b) at the PCC the same instant that the fault occurs, (c)-(d) at the same instant of the fault mono-phase and more detailed (red, equivalent feeder).

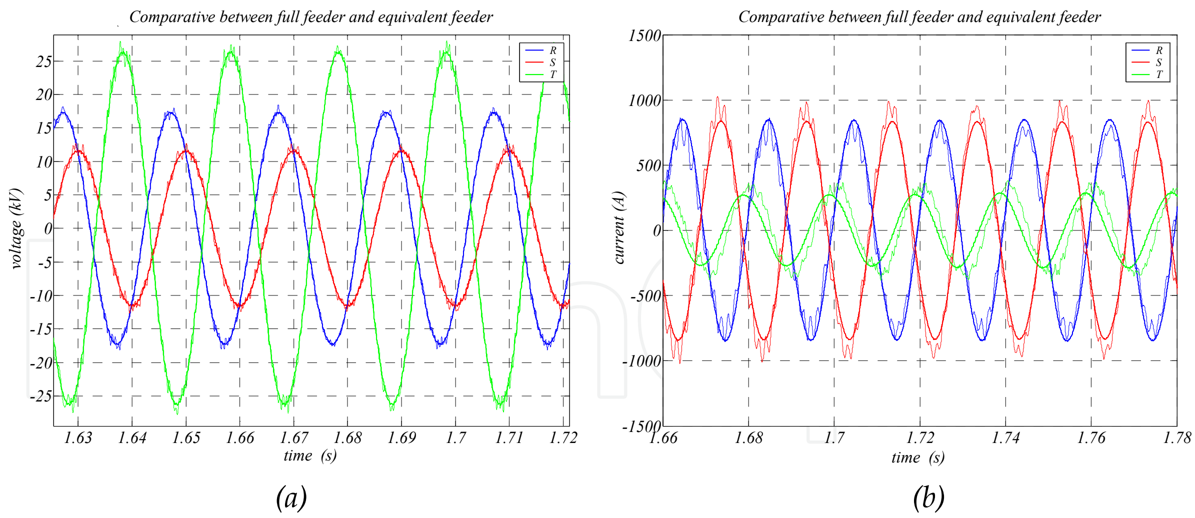

Figure F.10 Comparison of the equivalent wind turbine and the full feeder for a two-phase fault, the voltage (a) and current (b) at the PCC during the maintenance of the fault.

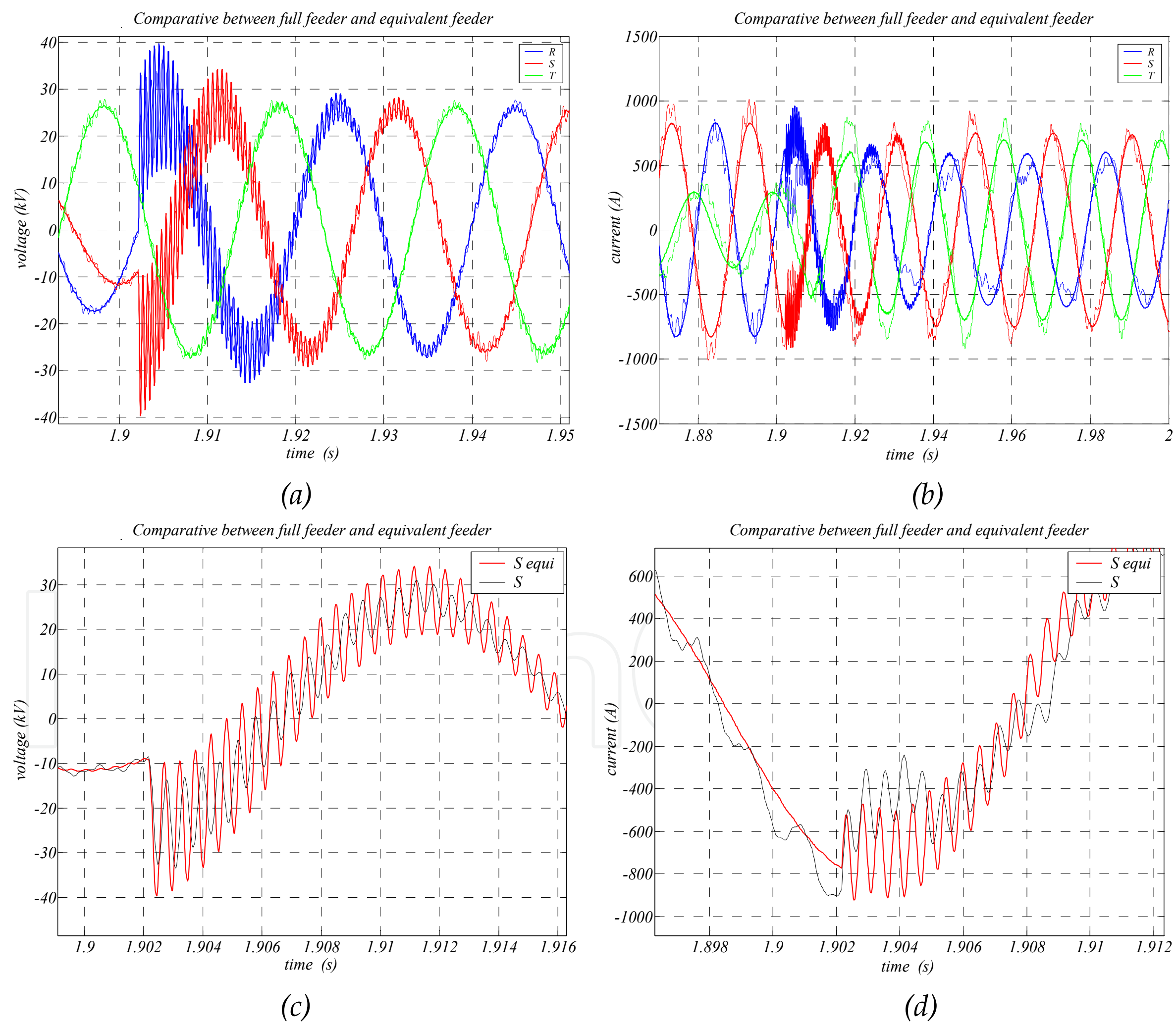

Figure F.11 Comparison of the equivalent wind turbine and the full feeder for a two-phase fault, the voltage (a) and current (b) at the PCC when the clearance of the fault occurs. (c)-(d) the voltage and current at the clearance of the fault mono-phase and more detailed, (red, equivalent feeder).

As is explained before, the transient response exhibits the typical behavior for a fault in a RLC circuit described in section 7.1. With regards to the frequency of the oscillation, the energy exchange between capacitive component of the cable and the short circuit impedance of the grid causes the oscillation. Therefore, this frequency depends on those impedances.

This fact (the dependence of the resonance and the oscillation frequency with the capacitive component / the total length of the inter-turbine grid) strengthens the decision to simplify the wind farm with equivalent wind turbines for each feeder and not only one. Because, using only one equivalent wind turbine for the entire wind farm, with only an equivalent inter-turbine cable (less capacitive component), will change this oscillation frequency.

Obviously, the simplification carried out also changes the oscillation frequency and the de-energizing current peak for the cable, due to the fact that only takes into account a part of the inter turbine cable (equation (144)), not the whole cable. But, is better simplification than only one equivalent wind turbine which takes into account only a very little part of the total capacitive component of the real inter-turbine grid.

Looking to the results obtained in both scenarios, it is possible to see a similar oscillation frequency and a reasonable similar current/voltage peaks. Moreover, roughly the evolution of the voltage and current are similar too. Thus, based on the results depicted in Figure F.2 - Figure F.6 and Figure F.7 - Figure F.11, it is possible to conclude that the equivalent wind turbine is a reasonable accurate simplification.

Appendix G: Considered STATCOM Model to Validate the Proposed Solution

The objective of the present appendix is to characterize the model and characteristics of the considered STATCOM used in the simulation scenario to validate the proposed electric connection infrastructure (chapter 7, section 7.5.4).

This simulation is oriented mostly to measure the injected reactive power by the offshore installation to the main grid (at the PCC). Therefore, the most important characteristic of the STATCOM is its rated current/power, i.e. the capability of the STATCOM to inject reactive power during voltage dips at the PCC. Due to this fact, the details of the model and control of the STATCOM are not much relevant.

In this way, for the sake of simplicity, there are considered similar features for the STATCOM and for the grid side converters of the wind turbines: Same topology for the converter (a three-level topology with a 3.3kV ($v_{statcom}$) output voltage based on IEGTs, see section 5.2.2.1), same control strategy (two proportional-integral gains in the *d-q* frame for each sequence with cross-coupled terms, see section 5.2.2.2) and the same parameters to tune the LC-L filter (see section 5.2.2.3).

Thus, the considered STATCOM used in the simulation scenario to validate the proposed electric connection infrastructure is shown in Figure G.1.

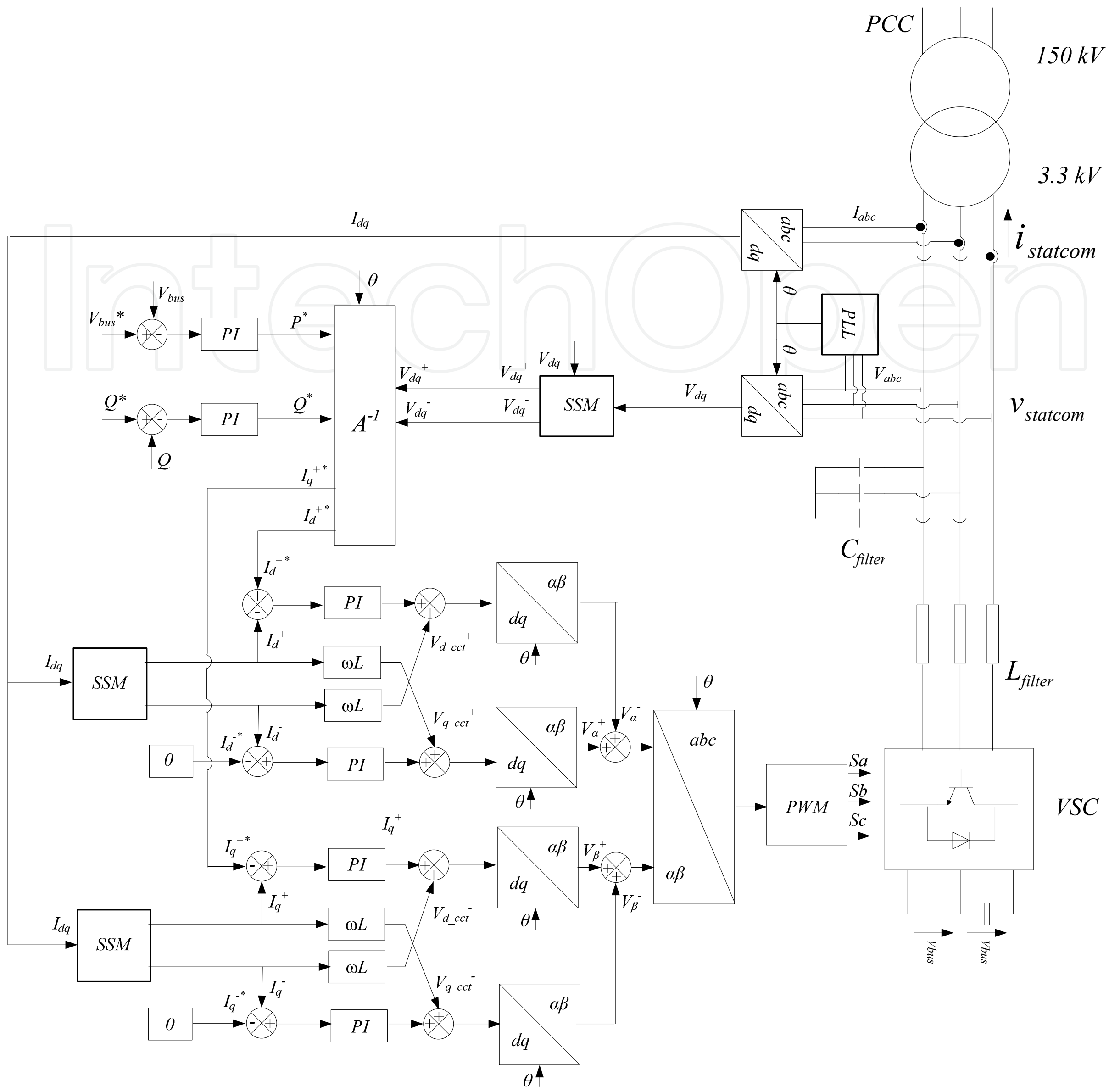

Figure G.1 Main scheme of the considered STATCOM used to validate the proposed electric connection infrastructure.

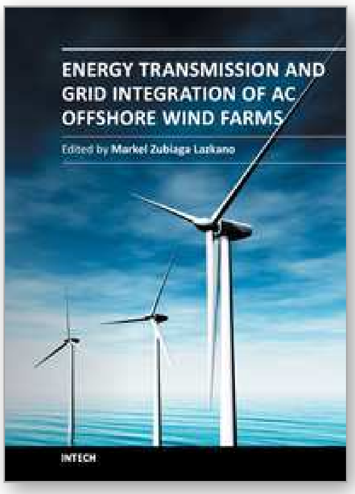

Energy Transmission and Grid Integration of AC Offshore Wind Farms
Edited by MSc Markel Zubiaga

ISBN 978-953-51-0368-4
Hard cover, 248 pages
Publisher InTech
Published online 21, March, 2012
Published in print edition March, 2012

This book analyses the key issues of the offshore wind farm's energy transmission and grid integration infrastructure. But, for this purpose, there are not evaluated all the electric configurations. In the present book is deeply evaluated a representative case. This representative case is built starting from three generic characteristics of an offshore wind farm: the rated power, the distance to shore and the average wind speed of the location. Thus, after a brief description of concepts related to wind power and several subsea cable modeling options, an offshore wind farm is modeled and its parameters defined to use as a base case. Upon this base case, several analyses of the key aspects of the connection infrastructure are performed. The first aspect to analyze is the management of the reactive power flowing through the submarine cable. Then, the undesired harmonic amplifications in the offshore wind farms due to the resonances and after this, transient over-voltage problems in the electric infrastructure are characterized. Finally, an offshore wind farm connection infrastructure is proposed in order to achieve the grid code requirements for a specific system operator, but not as a close solution, as a result of a methodology based on analyses and simulations to define the most suitable layout depending on the size and location of each offshore wind farm.